Hydrobiologia (2009) 620:47–61
DOI 10.1007/s10750-008-9614-7

PRIMARY RESEARCH PAPER

Phytoplankton distribution and production along a wide environmental gradient in the South-West Atlantic off Uruguay

Danilo Calliari · Ernesto Brugnoli · Graciela Ferrari · Denise Vizziano

Received: 7 April 2008 / Revised: 18 September 2008 / Accepted: 20 September 2008 / Published online: 4 October 2008

Abstract We investigated phytoplankton biomass, assemblage structure and production along an environmental gradient to evaluate if chlorophyll-*a* (as proxy for biomass) and primary production peaked under conditions hypothesised to favour phytoplankton growth. During Spring 2003, a wide area from shallow estuarine waters to the shelf slope off the Río de la Plata was sampled and routine measurements included CTD profiles, nutrients, chlorophyll-*a*, phytoplankton composition and abundance, seston and organic matter loads, downwelling light and, at selected stations, production versus irradiance experiments. Spatial differences in abiotic variables suggested distinct hydrographic zones that differed in phytoplankton biomass and productivity. Chlorophyll-*a* was highest under estuarine influence and peaked at low salinity when strong stratification developed in the outer estuary, and was minimum at the shelf break and slope. In that area, however, relatively high chlorophyll-*a* was associated to oceanographic fronts and to the occurrence of Sub Antarctic water within the photic depth range. Productivity was maximum in shallow waters, but biomass-specific productivity peaked at the outer shelf in oceanographic fronts or in upwelled Sub Antarctic waters. Over shelf and slope waters productivity and biomass were not tightly coupled, as indicated by situations of high biomass and low productivity (Station 9), low biomass and high productivity (Station 10), or both high biomass and productivity (Station 22). Ordination analysis of phytoplankton taxa suggested that assemblages changed gradually along the environmental gradient and correlated to abiotic variables defining geographic zones. Overall results were consistent with an interpretation that phytoplankton biomass and growth were modulated by light in estuarine and coastal waters, and by hydrographic processes on the continental shelf and slope.

Keywords Phytoplankton · Chlorophyll · Primary production · Southwest Atlantic · Río de la Plata · Uruguay

Handling editor: Luigi Naselli-Flores

D. Calliari (✉) · E. Brugnoli · D. Vizziano
Sección Oceanología, Facultad de Ciencias, Universidad de la República, Iguá 4225, CP 11400 Montevideo, Uruguay
e-mail: dcalliar@fcien.edu.uy; danilo.calliari@marecol.gu.se

D. Calliari
Sven Lovén Centre for Marine Research-Kristineberg, Marine Ecology Department, Göteborgs University, Kristineberg 566, 450 34 Fiskebäckskil, Sweden

G. Ferrari
Dirección Nacional de Recursos Acuáticos, Constituyente 1497, CP 11200 Montevideo, Uruguay

Introduction

Production and fate of organic matter in marine ecosystems are modulated to a large extent by physical

processes (Platt et al., 2005; Mann & Lazier, 2006). The selection of phytoplankton life forms under contrasting conditions has strong implications for the pathways and efficiency of organic matter and energy transfer to large-sized consumers (Kiørboe, 1993; Mann & Lazier, 2006). High biological production at different trophic levels in the marine environment, including fisheries, can be generally traced back to characteristic oceanographic processes, i.e. coastal upwelling, tidal or shelf-break fronts, seasonal thermocline formation, among others.

Coastal and oceanic waters off Uruguay host environments with contrasting physical, chemical and biological characteristics. Along a coast–ocean gradient there is an estuarine dominated zone whose influence extends over the inner shelf (up to ca. 50-m depth), and further offshore the Subtropical Convergence (SC) dominates on shelf and slope waters. This region is an important CO_2 uptake area in the global C budget, particularly during austral spring and summer (Feely et al., 2001; Bianchi et al., 2005). Planktonic production at estuarine, shelf and slope ecosystems sustains important fisheries by littoral states Argentina, Brazil and Uruguay, as well as from international fleets (Bisbal, 1995).

The Río de la Plata (RP) estuary represents the main point source of freshwater in the South Atlantic (Boltovskoy et al., 1999). Capital cities Buenos Aires and Montevideo on opposite banks of RP are home to >15 million people and to large industrial and harbour facilities; coastal waters are intensively used for seemingly conflicting purposes like drinking water supply, waste water and sewage sink, shipping, angling and commercial trawling, tourism and recreation, all of which mount strong environmental pressures on the ecosystem (Wells & Daborn, 1997; CARP-CTMFM, 1999; Nagy et al., 2002).

In spite of intense use research effort has been scarce and knowledge of basic ecological aspects of coastal and open waters—like phytoplankton distribution and primary production levels—is very limited or non-existent. Earlier studies focused on phytoplankton distribution in the estuarine area (Calliari et al., 2005), continental shelf outside the RP (Carreto et al., 1986; Negri et al., 1988) and frontal eddies in the SC (Gayoso & Podestá, 1996; Garcia et al., 2004). Carreto et al. (2003) described the taxonomic structure and detailed pigment signatures of phytoplankton assemblages in surface waters along an estuarine–oceanic gradient. Also, a large-scale latitudinal transect in offshore waters evidenced clear hydrographic, chemical and biological (chlorophyll-*a*) differences associated to alternating dominance of Brazil and Malvinas Currents on the SC region (Brandini et al., 2000). North of the RP Hubold (1980) and Ciotti et al. (1995) found that freshwater outflow modulated the nutrient content of coastal waters when mixed with subtropical water (STW) and sub Antarctic water (SAW), and promoted higher chlorophyll-*a* levels on the Southern Brazilian Shelf. However, no attempt has been done so far to explore phytoplankton responses to environmental variability on a synoptic scale from estuarine to deep areas off the RP.

In particular, there is a remarkable scarcity of studies exploring vertical distribution patterns of phytoplankton biomass, although valuable exceptions exist (Carreto et al., 1986; Ciotti et al., 1995; Brandini et al., 2000). These patterns can be characteristic for large marine areas (Platt et al., 2005) and an important factor determining the potential for primary production (PP). Given that remote sensing of chlorophyll-*a* in marine waters is restricted to a thin uppermost layer, the relationship between surface phytoplankton biomass and that in the entire euphotic layer results of great relevance for modelling PP from remote sensing data (Platt et al., 2005; Yacobi, 2006). Also, although evidence from sea–atmosphere CO_2 fluxes suggest high PP associated to frontal structures (Feely et al., 2001; Bianchi et al., 2005), no measurements exist for this large marine area.

The present study was set to characterise a large-scale gradient between the RP and the shelf-brake off Uruguay in terms of environmental variables, phytoplankton biomass, assemblage composition and primary production. The main goal was to evaluate if distribution of phytoplankton biomass and production differed between zones and peaked under conditions hypothesised to favour phytoplankton growth, and to explore the correlation between assemblage structure and environmental variables.

Materials and methods

Study area

The RP is a shallow and large-scale estuary at ca. 34°10′–36°20′S and 55°00′–58°30′W, which drains

the second largest basin in South America; it is ca. 230-km wide at the mouth and <20-m deep, with a mean annual flow of ca. 23,000 m^3 s^{-1} (Framiñán & Brown, 1986). The RP outflow modulates salinity distribution over the inner continental shelf and can be traced as a low salinity plume extending as far as 28°S (Piola et al., 2000). Over the shelf break the SC results from the collision of warm, southward Brazil Current (BC) and the cold Malvinas Current (MC = Falkland Current) flowing northwards. The SC area is broadly located over the shelf break and offshore between 32°S and 40°S (average position centred at ca. 38°S), where highly energetic mixing dynamics result in complex frontal systems and hydrographic structures like eddies and meanders. Subsequent to collision, the MC loops backwards forming the Malvinas Return Flow, while the BC is deflected in a North–East direction at ca. 44°S (Saraceno et al., 2005). Brazil and Malvinas waters have contrasting termohaline signatures and dissolved nutrients levels, the former being warmer, saltier and oligotrophic in relation to the latter.

Field sampling

Biological and physical sampling was performed during spring 2003 at 28 stations in three transects during two successive cruises (Fig. 1). Transect 1 comprised 17 Stations (Stations 1–17) along a NW–SE transect that covered the whole range of environments

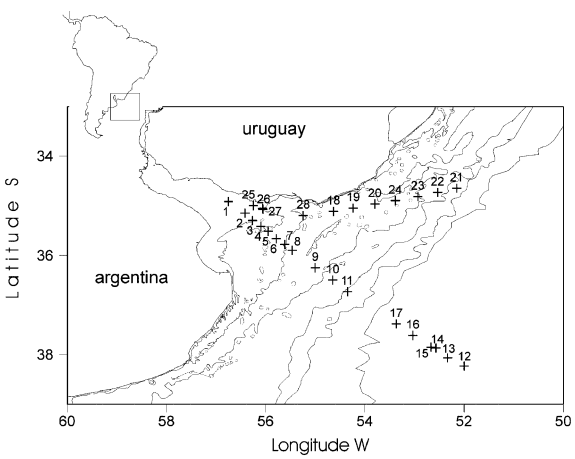

Fig. 1 Map of the study area showing location of sampling stations during the three cruises and corresponding station numbers. Contour lines denote 10, 20, 50, 100, 200 and 1,000 m isobaths

from shallow estuarine to deep waters on the shelf slope (depth range ca. 6–4,500 m) sampled between December 11th and 15th; transect 2 was oriented WSW-ENE and comprised seven Stations (Stations 18–24) on the Uruguayan shelf up to the shelf break (depth range 30–150 m) sampled on December 16th and 17th. Transects 1 and 2 were completed on board R/V Aldebarán. Transect 3 comprised four Stations (Stations 25–28) within the Uruguayan estuarine and shallow coastal area (depth range ca. 8–20 m), and was sampled on November 20th on board R/V Akademik Vavilov.

Routine measurements included conductivity and temperature profiles with Neil Brown (R/V Vavilov) and Sea Bird SBE 19 (R/V Aldebarán) CTD probes, and downwelling photosynthetic active radiation (PAR) measured with a LiCor LI250 fitted with a 2π quantum sensor. Salinity measurements derived from conductivity readings correspond to the practical salinity scale and are reported without units. Bottle samples were taken at five depths for measuring seston load (total particulate matter in suspension), particulate organic matter (POM, the organic fraction of seston), dissolved inorganic macronutrients (PO_4-P, NO_3 + NO_2-N and SiO_2-Si) and chlorophyll-*a* concentration, and for phytoplankton identification and counting. Quantitative phytoplankton samples were preserved in acid Lugol solution. Also, qualitative phytoplankton samples were taken by horizontal surface tows of a 25 μm pore size conical net, and preserved in 4% formaldehyde. For seston and POM between 200 and 1,000 ml of water (according to seston content) were filtered through pre-combusted and pre-weighted GF/F filters (nominal pore size 0.7 μm) and stored at −20°C until analysis. For chlorophyll-*a* estimation aliquots of 0.1–1 l were filtered onboard through GF/F filters in quadruplicate and stored in liquid nitrogen.

At selected Stations (Stations #1, 5, 7, 9, 10 and 15 corresponding to transect 1, and Stations #18 and 22 corresponding to transect 2) primary production estimates were performed using the ^{14}C incorporation method (Steeman-Nielsen, 1952). Subsurface water samples were incubated on-deck under natural light in a simulated light gradient that comprised 10 PAR levels achieved by using neutral density screens (range 100–0.5% of surface irradiance); incubations started between 10:00 and 14:00 h local time and were run in triplicate clear and dark 120 ml DBO

bottles in a circulating bath at in situ surface water temperature. After 4 h, the experiment was finished by adding 1 ml of neutral analytic-grade formaldehyde 40%, and an aliquot of 5 ml was taken from each bottle and stored in 20 ml scintillation vials until laboratory analyses.

Laboratory methods

For chlorophyll-*a* measurement filters were placed in small vials and pigments extracted in 90% acetone for 24 h in the dark at 4°C. Chlorophyll-*a* concentration in the extracts from two of four replicates was derived from absorbance measurements in a VARIAN Cary-50 spectrophotometer according to Jeffrey & Humphrey (1975); in remaining replicates chlorophyll-*a* was measured with a Luminescence Spectrometer AMINCO Bowman Series 2 spectrofluorometer calibrated against standard chlorophyll-*a* solution (Sigma®, C5753). Dissolved SiO_2-Si was quantified according to Koroleff (1983) using a Beckman UV-26 spectrophotometer, and samples for PO_4-P, $NO_3 + NO_2$-N were run in a Foss-Tecator 5012 autoanalyser equipped with a FS 5027 sampler and a FS 5042 detector set for detection limits of 0.7 µM for PO_4-P and 7 µm for $NO_3 + NO_4$-N. That configuration was appropriate for estuarine high nutrient waters, but resulted in too high detection limits for several samples from deeper stations; those results should thus be taken cautiously. Seston and POM were estimated gravimetrically as the weight of the sample after drying (seston) and combustion (POM) following Strickland & Parsons (1972), and expressed as mg l^{-1}. Incorporation of ^{14}C was measured in a Beckman L16800 scintillation counter after acidification with 1 N HCl and addition of 5 ml of aqueous scintillation cocktail (BCS Amersham Biosciences).

Taxonomic determinations were carried out with MO Olympus or Diaplan Leitz microscopes at 1,000× magnification for cells down to a size of ca. 3 µm. Identification of diatoms was based on the oxidation technique (Hasle & Fryxell, 1970); plates of armed dinoflagellates were disarticulated using sodium hypochloride and stained with Lugol solution. The entire phytoplankton community was identified to species or genus level following proper references (i.e., Balech, 1988; Tomas, 1995).

Cell counts were made under inverted microscope by settling 10, 25 or 50 ml subsamples in Utermöhl chambers (Sournia, 1978). At least 100 cells of all dominant species were counted (error < 20%, Lund et al., 1958). Detailed analysis of phytoplankton taxonomy and species distribution is in progress (G. Ferrari), and results presented here correspond to surface samples.

Data analysis

Primary production versus irradiance data were assessed following Platt et al. (1980) and Harrison & Platt (1986). A general zonation pattern of the abiotic environment was assessed by non-metric multidimensional scaling (n-MDS, Field et al., 1982; Clarke & Warwick, 1994) and cluster analyses based on a Euclidean Distance matrix calculated from square root-transformed data. These analyses are similar (i.e. both are based on the same distance matrix), but provide complementary information: MDS provides a direct and objective representation of multivariate distances on a plane (or in a 3 D space); on the other hand, an objective delimitation of boundaries to define groups of similar cases is not straightforward on the MDS plane, but can be performed by cluster analysis. In the present case groups of stations were defined using a distance threshold value equal to the average of the Euclidean distance matrix (Arancibia, 1988; Rodríguez-Graña & Castro, 2003). The variables considered in these analyses were: salinity, temperature, seston, photic depth, density gradient between surface and photic depth, $NO_3 + NO_2$ and SiO_2; in order to avoid strong co-linearity a pre-screening excluded variables PO_4 and POM. Stations 13 and 14 were CTD-only and thus not considered in this analysis. Photic depth (Z_F) was defined as that at which light intensity was 1% of surface irradiance, and estimated as

$$Z_F = \frac{\mathrm{Ln}(0.01)}{k_d}$$

where k_d (m^{-1}) is the light extinction coefficient obtained from linear regression of log-transformed PAR versus depth. Analogous n-MDS analysis was performed on phytoplankton species abundance data to provide a description of spatial taxonomic variability; in this case a Bray–Curtis distance matrix (Clarke & Warwick, 1994) was calculated from abundance data transformed as $\log_{10}(x + 1)$; rarer taxa present in very low abundance (<0.1% calculated over all

samples) were not considered for this analysis. Relationship between environmental and biological data was evaluated by weighed Spearman rank correlation analysis of corresponding similarity matrices (Clarke & Ainsworth, 1993). The combination of environmental variables that yield maximum correlation between datasets was considered the best 'explanation' for the observed distribution, and significance of the correlation was tested by random permutation under the null hypothesis of no relation between multivariate patterns from the two sets of samples.

In order to assess if phytoplankton biomass differed between environments (hydrographic clusters) a one-way ANOVA was performed for dependent variables: surface chlorophyll-*a* concentration (Chl_0, mg m^{-3}), total chlorophyll-*a* integrated over the photic depth (Chl_F, mg m^{-2}), and depth-averaged Chl_F (Chl_F*, mg m^{-3}) estimated as Chl_F/Z_F. Prior to the ANOVA variables were $\log_{10}$-transformed and homocedasticity checked by Cochrane, Hartley and Bartlett test. Post-hoc differences between clusters were evaluated with Tukey HSD test (Honest Significant Difference) for unbalanced designs.

Finally, the relationship between surface Chl_0 (0–2-m depth) and Chl_F, was explored using forward stepwise multiple regression analysis; that allowed to assess if variables potentially available with space coverage comparable to surface chlorophyll-*a* as derived from remote sensors could assist in the estimation of integrated Chl_F. Predictive (independent) variables explored in this analysis were Chl_0, surface temperature, surface salinity and total water column depth.

Results

Environmental variables

Overall salinity ranged between <1 and full-strength sea water (36.43). Minimum temperature recorded was 4.38°C and maximum was 21.26°C; temperature–salinity signatures evidenced distinct water masses, including the very low salinity Río de la Plata waters (RPW) (Fig. 2). Non-metric MDS and cluster analyses on physical variables separated five groups that, with few exceptions, corresponded to recognizable areas: innermost estuarine (cluster #3), estuarine transition (cluster #5), shallow shelf (cluster #4), outer shelf (cluster #2) and oceanic (cluster #1) (Fig. 3); Station 1 was dominated by highly turbid freshwater and did not join any group.

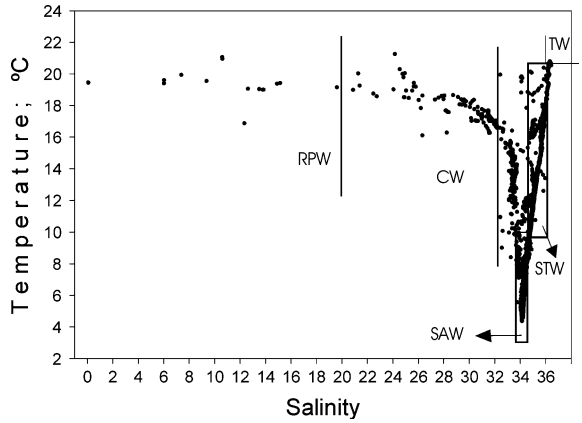

Fig. 2 Temperature–salinity plot corresponding to CTD casts performed during the three cruises in late spring. Lines within the plot represent termohaline limits of water masses as defined in the text: TW, tropical water; STW, subtropical water; SAW, Sub Antarctic water; CW, Coastal water; RPW, Río de la Plata water

Transect 1 presented most contrasting conditions. The influence of brackish RP waters along the first 296 km of transect 1 induced vertical salinity differences, which were strongest (up to 9.012 m^{-1}) in near-surface layers at Stations 9 and 10 (Fig. 4). Temperature decreased offshore until ca. Station 9, but tended to increase after Station 17. Coherent salinity and temperature fields evidenced two cores of relatively low salinity (<34.5) and low temperature water (<9°C), one over the shelf-brake centred 300 km offshore and at ca. 100-m depth, and a second at distances between 500 and 550 km at 50 m and deeper waters; these were separated by warmer (>14°C) and saltier (>34.5) waters, which also dominated near-surface layers from ca. 400 km offshore. Cores of SAW (Stations 11: >30 m, 13: >45 m) imbedded in STW indicated a branch of Malvinas current flowing northwards over the shelf break and a Malvinas return flow farther offshore. Concentration of dissolved nutrients was maximum in the estuarine region and decreased with distance from RP (Fig. 5); highest values recorded in near-surface waters were 33.9 µM for $NO_2 + NO_3$ (Station 4), 4.3 µM PO_4 (Station 6) and 118 µM SiO_2 (Station 1). Outside RP relative maxima occurred in subsurface and near-bottom waters of

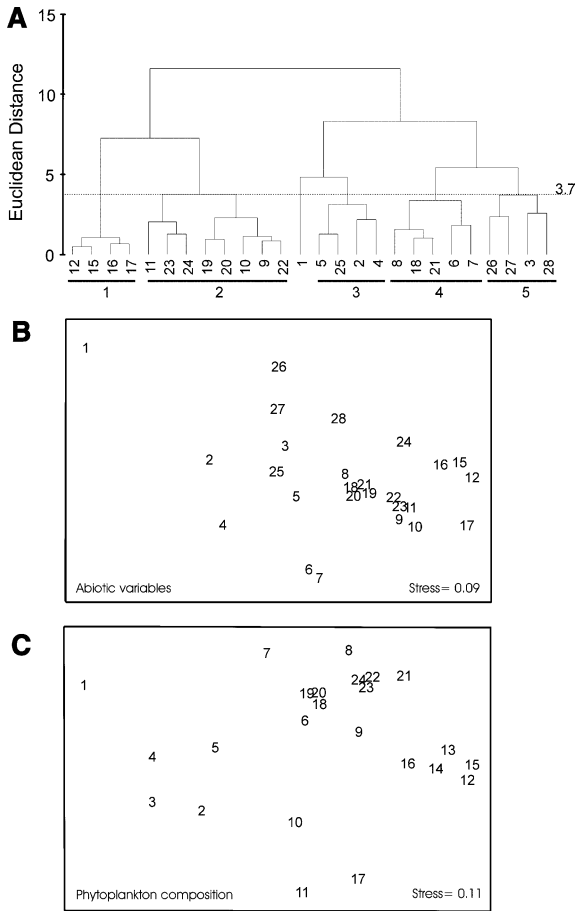

Fig. 3 **A** Cluster analysis and **B** non-metrical multidimensional scaling plot of stations based on Euclidean Distance similarity matrix of abiotic data. **C** Non-metrical multidimensional scaling plot of stations based on Bray–Curtis distance matrix of phytoplankton species abundance

the outer shelf, and in near-surface waters of oceanic Station 12 ($NO_2 + NO_3$); PO_4 levels were relatively high (>3 μM) on most stations, except surface waters at Stations 15 and 16; SiO_2 was low in near-surface waters (i.e. between 1 and 2 μM) except for moderately higher concentrations ca. 3–5 μM between Stations 16 and 17.

Transect 2 presented narrower ranges of temperature and salinity (Fig. 6). Salinity varied between 26.03 and 36.43, except for a local minimum (12.32) that occurred as a thin surface lens <2-m thick at Station 20. Outstanding features included a nucleus of relatively low salinity (<34) and low temperature water (<12.5°C) at 40–70-m deep between Stations 22 and 23; a core of warm (>19°C) and high salinity water (>36) was found in the offshore end of transect 2 (Station 21) between ca. 35 and 80-m depth. TW appeared only in subsurface levels (ca. 40–65 m) at the station farthest offshore (Station 21), separated from colder (likely SAW-influenced) waters by a sharp front between Stations 21 and 22. Higher $NO_3 + NO_2$ and PO_4 concentrations occurred at subsurface levels of Stations 19 and 20 (37 and 4.6 μM of $NO_3 + NO_2$ and PO_4, respectively), and in near-surface layers in Stations 23 and 24 (only nitrogen, Fig. 7). SiO_2 ranged between 15.96 μM at Station 18 and 0.43 at Station 23 (Fig. 7). As expected, values observed in transect 3 resembled those in the estuarine sector of transect 1 (Fig. 8).

Phytoplankton and relationship with environmental variables

Spectrophotometric and spectrofluorometric determinations of chlorophyll-*a* yielded equivalent concentration values as shown by linear regression: $\text{Chl}_{\text{espectro}} = b * \text{Chl}_{\text{fluo}}$ ($r^2 = 0.86$, $n = 132$, $P < 0.01$, $b = 0.96$ with 95% confidence limits 0.91–1.01). Both datasets were then pooled for further analyses. Chlorophyll-*a* in transect 1 ranged from 18.7 mg m^{-3} at Station 3 to <0.1 mg m^{-3} in surface levels of Station 16 and deep waters of shelf slope (Fig. 4); there was an offshore decreasing trend with an absolute maximum at Station 3, surface layers. Areas with relatively high chlorophyll-*a* included a subsurface maximum at Station 9 (2.45 mg m^{-3}, ca. 30 m), a near-surface region with levels between 0.79 and 1.5 mg m^{-3} between Stations 11 and 17, and a minor surface maximum slightly >1 mg m^{-3} at Station 13. In transect 2 chlorophyll-*a* was less variable between 0.39 and 3.61 mg m^{-3} (Fig. 6). There was no spatial pattern, but higher-than-average levels (i.e. 2 mg m^{-3}) occurred at Stations 19 (surface), 20 (surface and bottom) and 22 (20 m), while low chlorophyll-*a* areas (<1 mg m^{-3}) were found at Station 21, and partially at Stations 23 (from surface to 15-m depth) and 24 (between 15 and 20-m depth).

ANOVA indicated that clusters of Stations defined according to environmental variables differed in surface chlorophyll-*a* concentration (Chl_0) and in photic depth average chlorophyll-*a* (Chl_F*), but not in photic depth integrated chlorophyll-*a* (Chl_F, Table 1); inner estuarine stations (cluster 3) presented highest

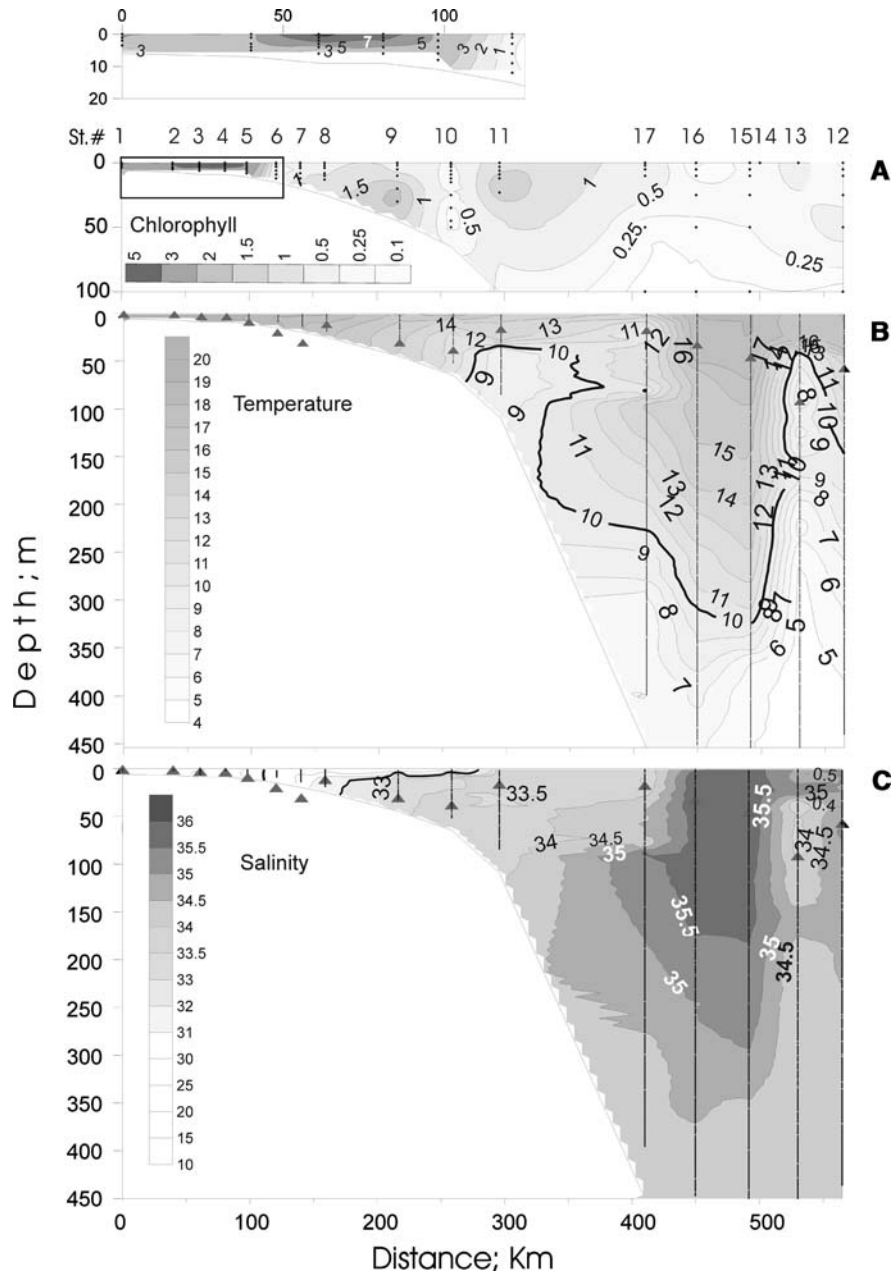

Fig. 4 **A** Chlorophyll-*a* (mg m^{-3}), **B** temperature (°C) and **C** salinity sections along transect 1. For chlorophyll-*a* blow-up section corresponding to first 125 km and up to 20-m depth is included on top. Black dots denote actual sample locations (distance, depth)

chlorophyll-*a*, and oceanic stations (cluster 1) lowest (Table 2). Stepwise multiple regression selected Chl_0 and surface salinity as explaining variable for Chl_F (Table 3).

Primary production evidenced photoinhibition responses at moderate and high-light intensity in all cases (Fig. 9). Highest maximum primary production rates (P_m, mg C m^{-3} h^{-1}) occurred in low salinity waters inside the estuary (Stations 1 and 5); but maximum biomass specific production (P^B_m, mg C μg Chl^{-1} h^{-1}) peaked in outer shelf waters (Stations 10 and 22), with intermediate values in estuarine waters and minimum over inner shelf areas (Stations 7, 9 and 18, Fig. 9).

A total of 134 phytoplankton taxa were identified in surface samples, distributed in nine classes Bacillariophyceae (57 taxa), Chlorophyceae (5), Cryptophyceae (9), Cyanophyceae (4), Dictyochophyceae (2), Dinophyceae (53), Prasinophyceae (1), Prymnesiophyceae (2) and Zygnematophyceae (1).

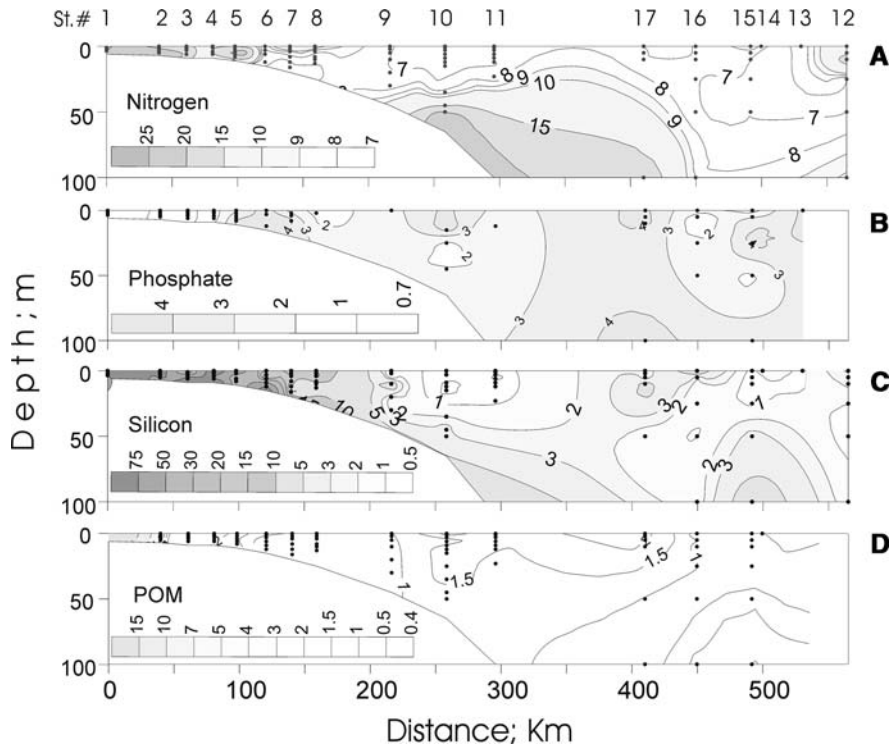

Fig. 5 **A** $NO_2 + NO_3$ (μM), **B** PO_4 (μM), **C** SiO_2 (μM) and **D** particulate organic matter (mg l^{-1}) sections along transect 1. Black dots denote actual sample locations (distance, depth)

Not surprisingly n-MDS ordination reflected similar patterns to that of abiotic variables (Fig. 3, Table 4): freshwater Station 1 was strongly dominated by colony-forming cyanophyceae *Microcystis aeruginosa* Kützing and appeared as a distinct case; estuarine Stations 2–5 showed moderate similarity among them, but were highly different from all others; inner and outer shelf Stations (18–24) were closely packed together and surrounded by estuarine transition Stations 6–9; deep oceanic Stations 12–16 also constituted a nucleus of highly similar cases, while Stations 10, 11 and 17 differed from most other assemblages and were characterised by a strong dominance of pico-cyanobacteria, picoplanktonic coccoids and a non-identified flagellate. There was a significant correlation between the distribution of phytoplankton assemblages and environmental variables (Spearman $r = 0.55$, $P < 0.01$), with *Salinity*, *Seston*, Z_F, SiO_2 as those which most contributed to "explain" taxa distribution.

Discussion

Stations sampled comprised contrasting environments: in all, five water masses were sampled according to temperature–salinity signatures (Sverdrup et al., 1942; Thomsen, 1962; Guerrero et al., 1997; Piola et al., 2000, 2005). TW and SAW, together with RPW have most contrasting termohaline characteristics, the remaining two resulting from mixing of either TW–SAW (STW), or from a combination of TW, SAW and RPW over shelf areas (CW). RPW is not formally defined and cannot be assigned to narrow salinity and temperature ranges; but based on representative data at climatological temporal scale (i.e.; Guerrero et al., 1997) and present results (Fig. 2) it can be regarded as that with salinity <20, thus restricting the definition of CW for the present work to that with salinity $20 < S < 33.2$. RPW was the only water mass present in Stations 1–4, and in Station 25 (except at near-bottom layers).

Vertical distribution of chlorophyll-*a*

Surface chlorophyll-*a* was a good indicator for total chlorophyll-*a* in the photic layer, but interestingly, estimation of total chlorophyll-*a* was improved by incorporating surface salinity data. While this result is preliminary and should be regarded cautiously due to the low number of data pairs involved, it seems promising for future use in large-scale productivity

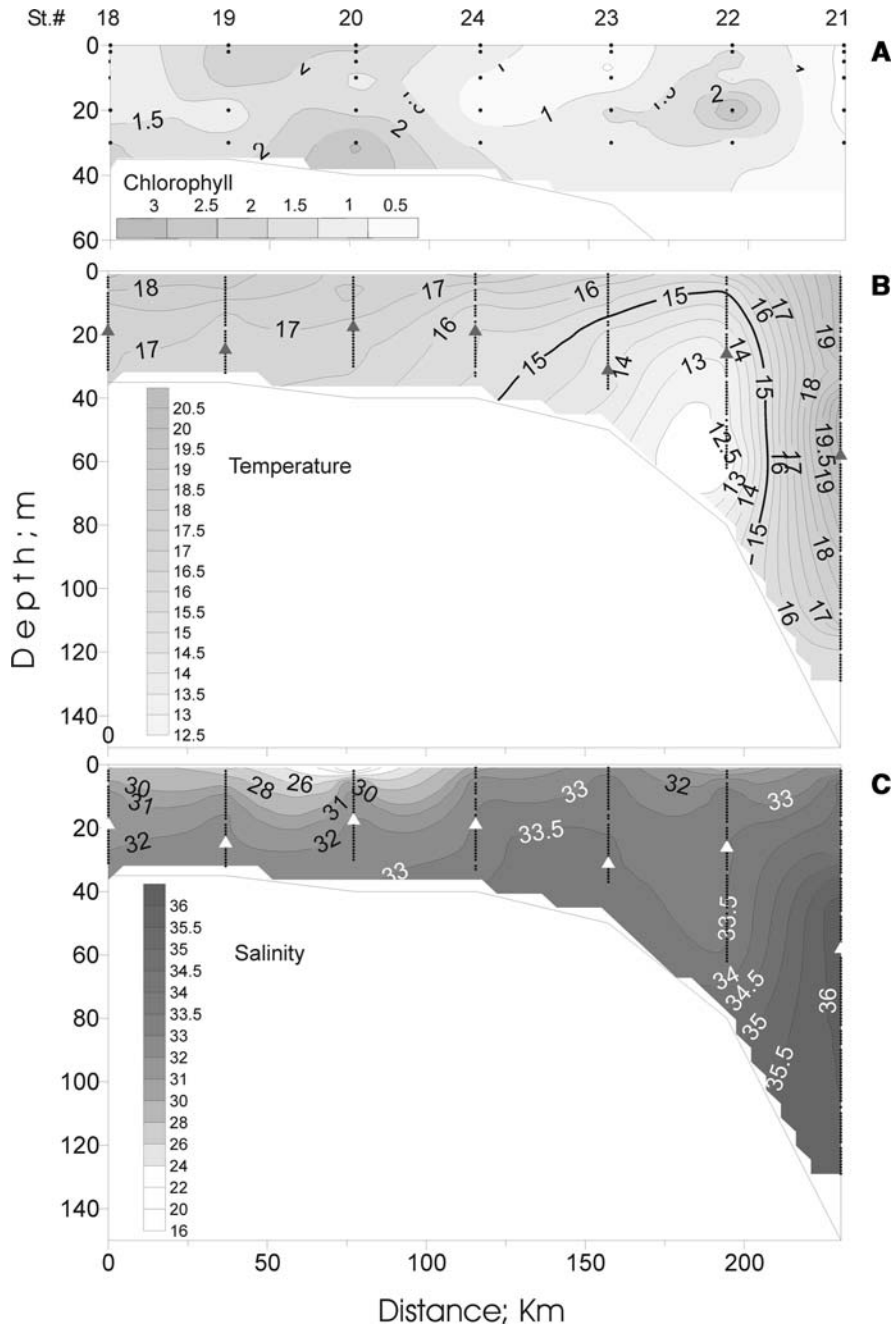

Fig. 6 **A** Chlorophyll-*a* (mg m^{-3}), **B** temperature (°C) and **C** salinity sections along transect 2. Black dots denote actual sample locations (distance, depth)

models based on remote sensing of chlorophyll-*a*, considering recent advances on salinity measurements from air-born sensors (Perez et al., 2006). One exception to that pattern was Station 20 where maximum chlorophyll-*a* occurred at 30 m, well below the photic depth. Such deep chlorophyll-*a* maximum may have represented an adaptation of cells to low-light conditions as indicated by eight times higher chlorophyll-*a* $cell^{-1}$ at 30 m compared to the average ratio for the four shallower depths (and ca. 2.5 times higher than at 20 m) at the same station.

Chlorophyll-*a* concentration in surface waters and depth-averaged chlorophyll-*a* over the photic layer differed between environmental areas (clusters)

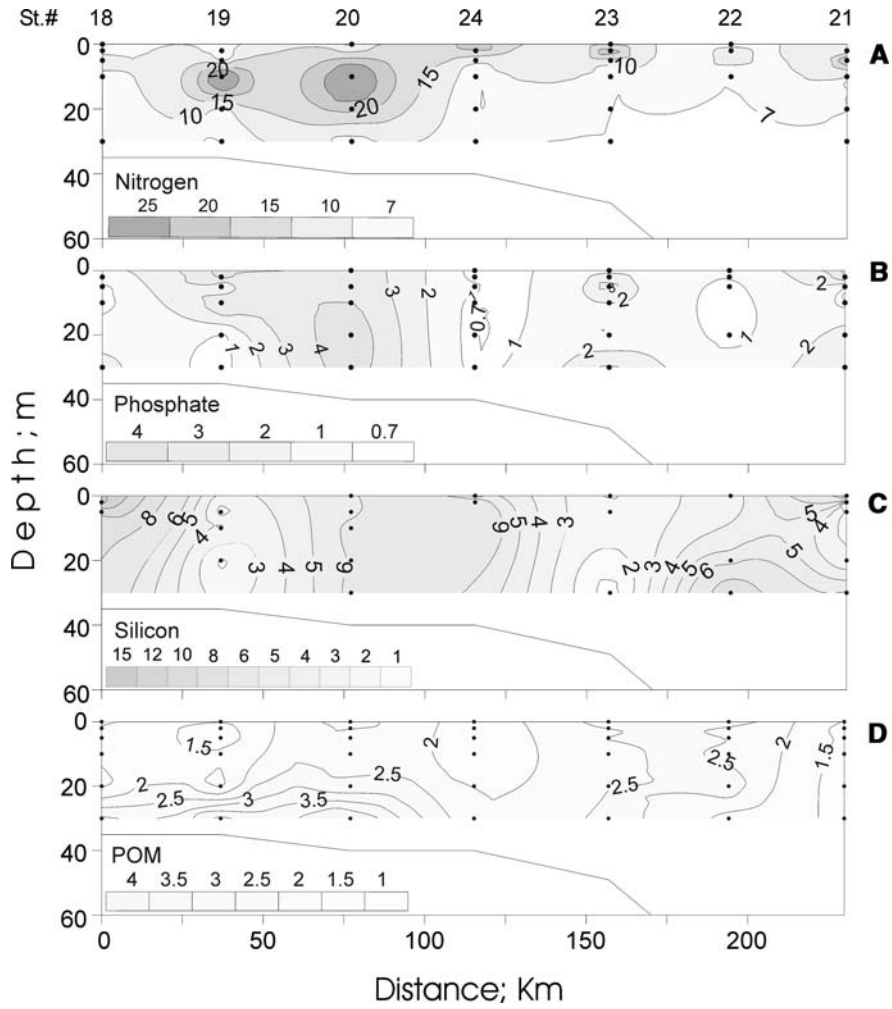

Fig. 7 **A** $NO_2 + NO_3$ (μM), **B** PO_4 (μM), **C** SiO_2 (μM) and **D** particulate organic matter (mg l^{-1}) sections along transect 2. Black dots denote actual sample locations (distance, depth)

defined according to abiotic variables. Such finding implies that differences in potential productivity between areas should also be expected, as further indicated by current primary production results. The structure of the phytoplankton assemblage, at least the micro- and nano-size fractions identified by direct microscopic observation, followed to a large extent the physical environment as indicated by: (i) similar distribution pattern of stations ordination on the MDS plane (Fig. 3); and (ii) significant correlation between respective distance matrices, where variables *Salinity*, *Seston*, Z_F, SiO_2 were most influencing on that correlation. Those results are largely consistent with earlier reports on the zonation of phytoplankton structure in the study area (Negri et al., 1988). Next, we discuss present findings on chlorophyll-*a*, primary production and phytoplankton distribution in relation to potential regulating mechanisms.

Río de la Plata and inner shelf

Cluster #3 grouped Stations with strongest influence of the RP (low salinity, and high seston load, k_d and nutrient concentration). Within the whole study area, the RP and transition stations (cluster #5) constituted the zone of highest chlorophyll-*a* levels. Here, chlorophyll-*a* reached the absolute maximum at surface Station 3, coincident with salinity ca. 7 and the establishment of strong stratification. In that area, RP Station 1, P–I response evidenced high biomass-specific production efficiency (parameter α) suggesting an assemblage adapted to low-light conditions (Harrison & Platt, 1986; Hill et al., 1995); the phytoplankton assemblage at the RP area was mostly represented by diatoms *Cryptomonas* sp. Ehrenberg, *Coscinodiscus radiatus* Ehrenberg, *Skeletonema tropicum* Cleve, and *Chaetoceros subtilis* Cleve.

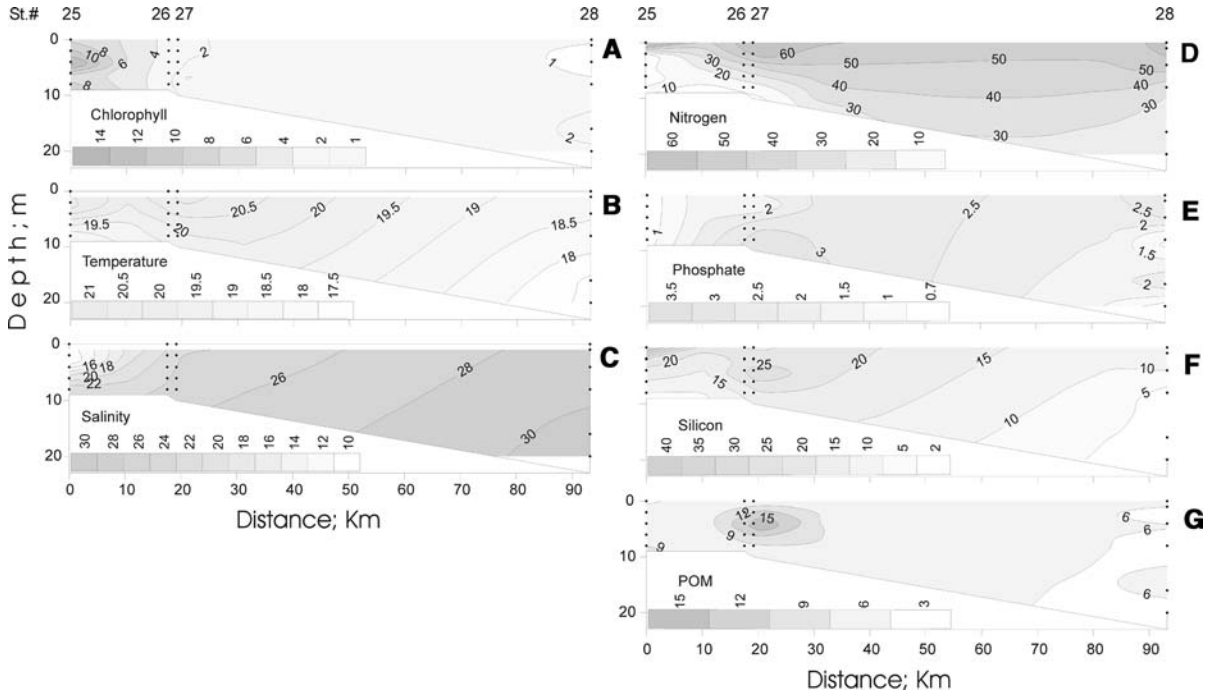

Fig. 8 **A** Chlorophyll-*a* (mg m^{-3}), **B** temperature (°C), **C** salinity, **D** $NO_2 + NO_3$ (μM), **E** PO_4 (μM), **F** SiO_2 (μM) and **G** particulate organic matter (mg l^{-1}) sections along transect 3. Black dots denote actual sample locations (distance, depth)

Table 1 Results of ANOVA performed to test for differences between clusters of stations in chlorophyll concentration

Effect	DF	*F*	*P*
Surface			
Intercept	1	10.4	0.004
Cluster	4	16.3	≪0.01
Error	20		
Total in photic depth			
Intercept	1	823.9	≪0.01
Cluster	4	1.8	0.17
Error	20		
Average concentration in photic zone			
Intercept	1	294.2	≪0.01
Cluster	4	17.8	≪0.01
Error	20		

Above: chlorophyll in surface layers; middle: total chlorophyll integrated over the photic zone; below: depth-averaged chlorophyll over the photic zone

Table 2 Results of Tukey HSD post-hoc test for differences in variables *surface chlorophyll-a concentration* (Chl_0, mg m^{-3}) and *average chlorophyll-a in the photic depth* (Chl_F, mg m^{-3}) among clusters of stations

Cluster	Chl_0		Chl_F	
	Mean value	Group	Mean value	Group
1	0.45	A	0.64	A
2	1.36	B, C	1.54	A, B
3	6.49	D	6.99	C
4	0.85	A, B	0.95	A
5	4.08	C, D	2.86	B

Letters A–D indicate homogeneous groups at $P < 0.05$. Previous ANOVA indicated significant differences between clusters for *surface chlorophyll-a concentration* ($F_{4,\ 20} = 16$, $P \ll 0.01$) and for average *chlorophyll-a in the photic depth* ($F_{4,\ 20} = 18$, $P \ll 0.01$)

At Station 5 parameter α decreased along with improved light conditions (i.e. lower seston load and k_d), while at Station 7 (cluster #4, inner shelf) P_m^B decreased, presumably indicating incipient nutrient limitation (MacCaull & Platt, 1977; see also Harding et al., 1982a, b); assemblage at Station 7 was dominated by coccoid cyanobacteria and nano-flagellates, besides diatoms in lower abundance (i.e., *Leptocylindrus* spp. Cleve). In accordance with earlier findings (Carreto et al., 1986; Calliari et al., 2005) those results strongly suggest that

Table 3 Results of multiple regression analysis on photic layer-integrated chlorophyll

Factor	B_n	SEB	t	P
Chl sup	17.62	4.63	3.80	$\ll$0.01
Salinity	0.37	0.15	2.38	<0.05

General model corresponds to: Chl_$Z_f = B_1$ * chl sup + B_2*salinity. SEB, standard error of B; t, Student's statistic; P, probability level. $N = 18$, $r^2 = 0.88$

phytoplankton growth was light limited in the highly turbid RPW, that light limitation was partly relieved by haline stratification and that nutrient limitation became the primary modulating factor in the inner shelf area next to the RP. Also, patterns of biomass distribution and primary production found in the present study support predictions of a physical–biogeochemical (NPZ) model for this ecosystem (Huret et al., 2005). The above interpretation largely

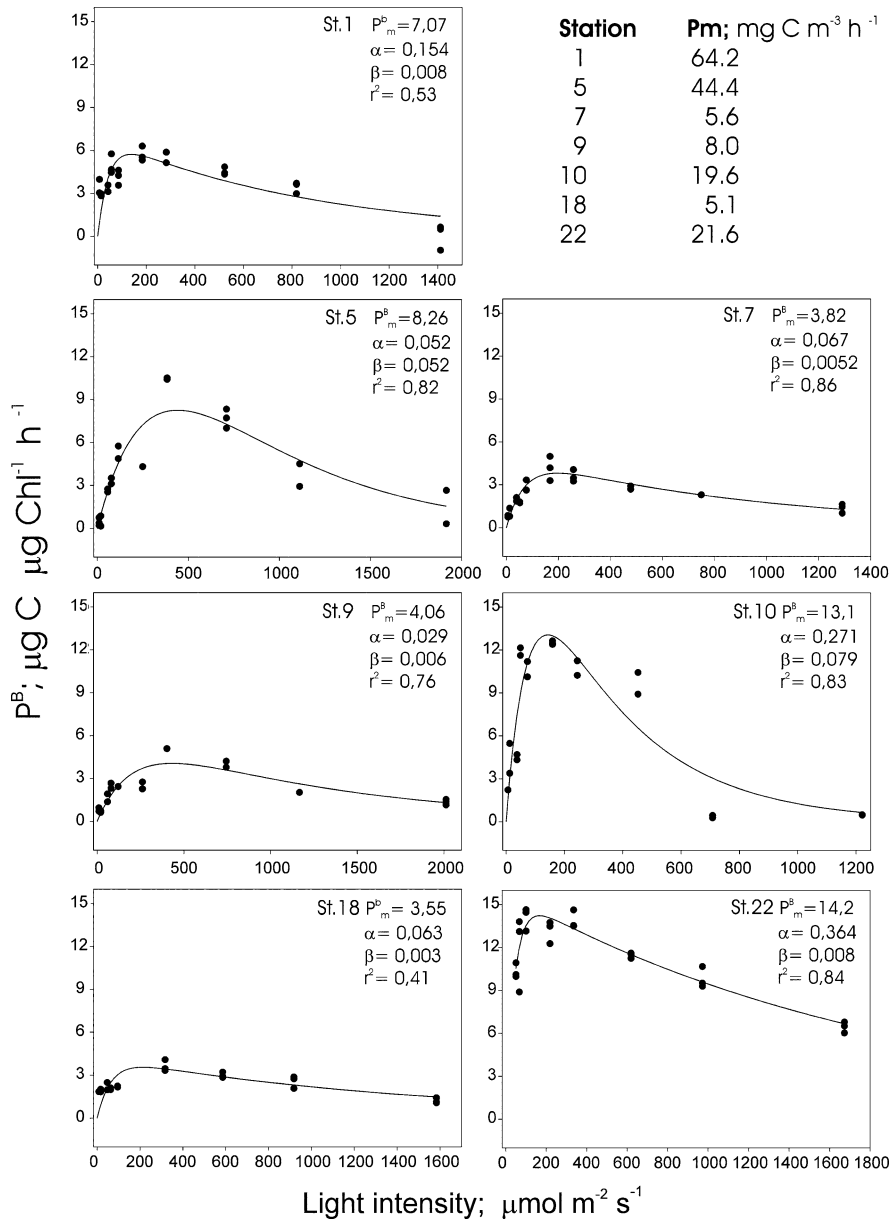

Fig. 9 Biomass-specific primary production (P^B, mg C µg Chl^{-1} h^{-1}) versus irradiance (mmoles m^{-2} s^{-1}) of sub-surface phytoplankton assemblages determined from ^{14}C incorporation during on-deck incubation experiments. Fitted parameters given for each case correspond to the photoinhibition response equation: $P_B = P_m^B \cdot \left(1 - e^{-\alpha \cdot I / P_m^B}\right) \cdot e^{-\beta \cdot I / P_m^B}$. Maximum production values estimated for each station are given in the inset at the upper-right corner. Results from experiment at Station# 15 presented no clear pattern and no model could be fitted to estimate response parameters; consequently data was judged unreliable and not further considered

Table 4 Representative phytoplankton of different areas within the region comprised by the Río de la Plata estuary and adjacent shelf and slope waters

Region	Representative taxa
Freshwater Station 1	*Microcystis aeruginosa*, *Skeletonema tropicum*, *Coscinodiscus radiatus*
Estuarine Stations 2–5	*Leptocylindrus* sp., *Skeletonema tropicum*, *Coscinodiscus radiatus*, *Chaetoceros subtilis*, *Cryptomonas* sp., Chlorophyta n.i.
Est-Shelf trans. Stations 6–9	*Actinocyclus normanii*, *Cerataulina pelagica*, *Coscinodiscus radiatus*, *Leptocylindrus danicus, L. minimus*, Cryptophyceae spp, Picocyanobacteria, *Karenia mikimotoi*
Shelf Stations 18–24	*Cerataulina pelagica*, *Chaetoceros subtilis*, *Leptocylindrus danicus*, *L. minimus*, *Leptocylindrus* sp., *Rhizosolenia pungens*, *Thalassionema nitzschioides*, *Prorocentrum micans*, Cryptophyceae spp
Shelf-brake Stations 10, 11 and 17	Picocyanobacteria, picoplanktonic chlorophyceae, Cryptophyceae spp, athecate dinoflagellates
Oceanic Stations 12–16	*Bacteriastrum delicatulum*, *Cerataulina pelagica*, *Leptocylindrus danicus*, *Navicula* sp., *Gyrodinium fusus*, Cryptophyceae spp

Phytoplankton was identified from surface samples only (Est, estuarine; trans., transition)

follows general concepts of production regulation in large-scale turbid estuaries (Wofsy, 1983; Pennock, 1985; Cloern, 1987, 1996, 1999; Grobbelaar, 1990), mainly developed for the San Francisco estuary and few other cases in the Northern Hemisphere. Present results suggest that such mechanisms may also be generalised to the RP, and that simple models based on light availability and biomass (Cole & Cloern, 1987) could provide synoptic estimates of primary production over ample regions of the estuary.

Shelf and shelf-break waters

The shelf and oceanic regions formed clusters #2 and #1, respectively, and were dominated by STW (primarily) and SAW (secondarily) water masses. TW occurred only marginally, and the transition between TW and colder waters marked a clear frontal structure (Stations 21 and 22); these fronts are expected sites of enhanced phytoplankton biomass (Hubold, 1980; Ciotti et al., 1995; Boltovskoy et al., 1999; Brandini et al., 2000) as earlier shown from remote sensing and in situ measurements (Gayoso & Podestá, 1996; Brandini et al., 2000; Garcia et al., 2004, 2005; Saraceno et al., 2005). Present results on biomass distribution and primary production supported that insight, and further suggested that near-surface occurrence of SAW favoured phytoplankton biomass development as well. Cluster #2 (outer shelf Stations) had highest chlorophyll-*a* levels outside the estuarine influence zone (Fig. 6, Table 1) and both elevated chlorophyll-*a* levels and production generally coincided with oceanographic situations where SAW (or waters under influence of SAW; i.e. temperature $10 < T < 15°C$) occurred within the euphotic depth range. Highest P^B values over the shelf and slope were associated to the thermal front in transect 2 (Station 22) and also with occurrence of SAW within the euphotic zone (Station 10); that constitutes the first direct evidence of enhanced growth under such conditions besides indirect estimations from bulk biomass (chlorophyll-*a*) or cell counts.

Interestingly, over shelf and slope waters phytoplankton productivity (P^B_m; μg C μg chl^{-1} h^{-1}) and biomass were not tightly coupled as shown by observations of concurrent high biomass and low productivity (e.g. Station 9), low biomass and high productivity (e.g. Station 10), or both high biomass and productivity (e.g. Station 22). Such de-coupling is no surprise given that productivity and actual biomass levels result of different mechanisms operating at dissimilar time-scales: productivity is a biomass-specific growth rate, which reflects physiological state of an assemblage at very short scales (i.e. minutes to hours), and is essentially dependent on growth conditions, i.e. light and nutrients availability, temperature, assemblage structure and taxa-specific rates. Biomass, on the contrary, results from the time integrated balance between past growth and loss processes, including sinking, grazing mortality, mixing and advection. Thus, proper understanding of mechanisms leading to actual productivity and biomass levels should consider potential time lags between onset of active primary production under favourable conditions and biomass build-up (analogous to the *shift up* in coastal upwelling systems;

Mann & Lazier, 2006), and the grazing pressure mainly by protozoan plankton (Strom et al., 2001; Calbet & Landry, 2004; Irigoien et al., 2006).

Thorough evaluation of both production and loss processes are thus in order for a mechanistic understanding of phytoplankton biomass distribution and dynamics; that is beyond the scope of the present study and constitutes a necessary next step in the investigation of this large marine area.

Acknowledgements We thank crews of R/Vs Aldebarán and Vavilov for assistance at sea, R. Piaggio (Montevideo City Municipality) for nitrogen and phosphorus analyses, and K. Sanz at Facultad de Ciencias (FC, Uruguay) for silicon analyses. V. García (FURG, Brazil), D. Conde and M. Gómez (FC) contributed with discussion of methods and D. Severov (FC) with discussion of physical oceanographic results. Research was funded by FEMCIDI-OAS 'Primera Iniciativa Trinacional del uso de mediciones radiométricas satelitarias de clorofila-a (SeaWiFS) en el área del Atlántico Sud-Occidental'. D. Calliari was supported by Marie Curie contract MIF1-CT-2005-007718 (European Commission) during writing of this manuscript.

References

Arancibia, H., 1988. Cluster Analysis. The Use of a Simple Statistical Method in the Identification of Groups. ICES Council Meeting (Collected Papers). ICES, Copehhagen, Denmark.

Balech, E., 1988. Los dinoflagelados del Atlántico Sudoccidental. Publ. Espec., Inst. Esp. Oceanogr., Ministerio de Agricultura, Pesca y Alimentación, Madrid.

Bianchi, A. A., L. Bianucci, A. R. Piola, D. Ruiz-Pino, I. Schloss, A. Poisson & C. F. Balestrini, 2005. Vertical stratification and air-sea CO_2 fluxes in the Patagonian shelf. Journal of Geophysical Research 110: C07003.

Bisbal, G. A., 1995. The southeast South American large marine ecosystem. Marine Policy 19: 21–38.

Boltovskoy, D., M. J. Gibbons, L. Hutchings & D. Binet, 1999. General biological features of South Atlantic. In Boltovskoy, D. (ed.), Zooplankton. Backhyus Publishers, Leiden, The Netherlands: 1–42.

Brandini, F., D. Boltovskoy, A. Piola, S. Kocmur, R. Rodttgers, P. C. Abreu & R. Lopes, 2000. Multiannual trends in fronts and distribution of nutrients and chlorophyll in the southwestern Atlantic (30–62°S). Deep-Sea Research I 47: 1015–1033.

Calbet, A. & M. R. Landry, 2004. Phytoplankton growth, microzooplankton grazing, and carbon cycling in marine systems. Limnology & Oceanography 49: 51–57.

Calliari, D., M. Gómez & N. Gómez, 2005. Biomass and composition of the phytoplankton in the Río de la Plata: large-scale distribution and relationship with environmental variables during a spring cruise. Continental Shelf Research 25: 197–210.

CARP-CTMFM, 1999. Proteccion Ambiental del Rio de la Plata y su Frente Maritimo. WWW electronic document available at http://www.freplata.org/documentos/archivos/Documentos_Freplata/Documento_de_proyecto_web.pdf.

Carreto, J. I., R. M. Negri & H. R. Benavides, 1986. Algunas características del florecimiento del fitoplancton en el frente del Río de la Plata. I: Los sistemas nutritivos. Revista Investigación y Desarrollo Pesquero 5: 7–29.

Carreto, J. I., N. G. Montoya, H. R. Benavides, R. Guerrero & M. O. Carignan, 2003. Characterization of spring phytoplankton communities in the Rio de la Plata maritime front using pigment signatures and cell microscopy. Marine Biology 143: 1013–1027.

Ciotti, A. M., C. Odebrecht, G. Fillman & O. O. Möller, 1995. Freshwater outflow and Subtropical Convergence influence on phytoplankton biomass on the southern Brazilian continental shelf. Continental Shelf Research 15: 1737–1756.

Clarke, K. R. & M. Ainsworth, 1993. A method of linking multivariate community structure to environmental variables. Marine Ecology Progress Series 92: 205–219.

Clarke, K. R. & R. M. Warwick, 1994. Change in Marine Communities: An Approach to Statistical Analysis and Interpretation. Plymouth Marine Laboratory, Plymouth.

Cloern, J. E., 1987. Turbidity as a control of phytoplankton biomass and productivity in estuaries. Continental Shelf Research 7: 1367–1381.

Cloern, J. E., 1996. Phytoplankton bloom dynamics in coastal ecosystems: a review with some general lessons from sustained investigations of San Francisco Bay, California. Reviews of Geophysics 34(2): 127–168.

Cloern, J. E., 1999. The relative importance of light and nutrient limitation of phytoplankton growth: a simple index of coastal ecosystem sensitivity to nutrient enrichment. Aquatic Ecology 33: 3–16.

Cole, B. E. & J. E. Cloern, 1987. An empirical model for estimating phytoplankton productivity in estuaries. Marine Ecology Progress Series 36: 299–305.

Feely, R. A., C. L. Sabine, T. Takahashi & R. Wanninkhof, 2001. Uptake and storage of carbon dioxide in the ocean: the global CO_2 survey. Oceanography 14: 18–32.

Field, J. G., K. R. Clarke & R. M. Warwick, 1982. A practical strategy to analysing multispecies distribution patterns. Marine Ecology Progress Series 8: 37–52.

Framiñán, M. & O. Brown, 1986. Study of the Río de la Plata turbidity front. Part I: spatial and temporal distribution. Continental Shelf Research 16: 1259–1283.

Garcia, C. A. E., Y. V. B. Sarma, M. M. Mata & V. M. T. García, 2004. Chlorophyll variability and eddies in the Brazil–Malvinas Confluence region. Deep-Sea Research I 51: 159–172.

Garcia, C. A. E., V. M. T. Garcia & C. R. McClain, 2005. Evaluation of SeaWiFS chlorophyll algorithms in the Southwestern Atlantic and Southern Oceans. Remote Sensing of Environment 95: 125–137.

Gayoso, A. M. & G. P. Podestá, 1996. Surface hydrography and phytoplankton of the Brazil–Malvinas currents confluence. Journal of Plankton Research 18: 941–951.

Grobbelaar, J. U., 1990. Modelling phytoplankton productivity in turbid waters with small euphotic to mixing depth ratios. Journal of Plankton Research 12: 926–931.

Guerrero, R. A., E. M. Acha, M. Framiñan & C. Lasta, 1997. Physical oceanography of the Río de la Plata estuary, Argentina. Continental Shelf Research 17: 727–742.

Harding, Jr., L. W., B. B. Prézelin, B. M. Sweeney & J. L. Cox, 1982a. Diel oscillations of the photosynthesis–irradiance (P–I) relationship in natural assemblages of phytoplankton. Marine Biology 67: 167–178.

Harding, Jr., L. W., B. B. Prézelin, B. M. Sweeney & J. L. Cox, 1982b. Primary production as influenced by diel periodicity of phytoplankton photosynthesis. Marine Biology 67: 179–186.

Harrison, W. G. & T. Platt, 1986. Photosynthesis–irradiance relationships in polar and temperate phytoplankton populations. Polar Biology 5: 153–164.

Hasle, G. R. & G. A. Fryxell, 1970. Diatoms: cleaning and mounting for light and electron microscopy. Transactions of the American Microscopy Society 89: 469–474.

Hill, W., M. Ryon & E. Schilling, 1995. Light limitation in a stream ecosystem: reponses by primary producers and consumers. Ecology 76: 1297–1309.

Hubold, G., 1980. Hydrography and plankton off southern Brazil and Río de la Plata, August–November 1977. Atlântica 4: 1–22.

Huret, M., I. Dadoua, F. Dumasb, P. Lazureb & V. Garcona, 2005. Coupling physical and biogeochemical processes in the Río de la Plata plume. Continental Shelf Research 25: 629–653.

Irigoien, X., K. J. Flynn & R. P. Harris, 2006. Phytoplankton blooms: a 'loophole' in microzooplankton grazing impact? Journal of Plankton Research 27: 313–321.

Jeffrey, S. & W. Humphrey, 1975. New spectrophotometric equations for determining chlorophylls a, b, c1, c2, in higher plants and phytoplankton. Biochemie una Physiologie der Pflanzen 167: 191–194.

Kiørboe, T., 1993. Turbulence, phytoplankton cell size, and the structure of pelagic food webs. Advances in Marine Biology 29: 1–72.

Koroleff, F., 1983. Determination of silicon. In Grasshoff, K., M. Ehrhardt & K. Kremling (eds), Methods of Seawater Analysis, 2nd ed. Verlang Chemie, Weinheim: 174–183.

Lund, J. W. G., C. Kipling & E. D. Le Cren, 1958. The inverted microscope method of estimating algal numbers and the statistical basis of estimations by counting. Hydrobiologia 2: 143–170.

MacCaull, W. A. & T. Platt, 1977. Diel variations in the photosynthetic parameters of coastal marine phytoplankton. Limnology & Oceanography 22: 723–731.

Mann, K. H. & J. R. N. Lazier, 2006. Dynamics of Marine Ecosystems. Biological–Physical Interactions in the Oceans, 3rd ed. Blackwell Scientific Publications, Malden.

Nagy, G. J., M. Gómez-Erache, C. H. López & A. C. Perdomo, 2002. Distribution patterns of nutrients and symptoms of eutrophication in the Rio de la Plata River Estuary System. Hydrobiologia 475(476): 125–139.

Negri, R. M., H. R. Benavides & J. I. Carreto, 1988. Algunas características del florecimiento del fitoplancton en el frente del Río de la Plata. II: Las asociaciones fitoplanctónicas. Publicaciones de la Comisión Técnica Mixta del Frente Marítimo 4: 151–161.

Pennock, J. R., 1985. Chlorophyll distribution in the Delaware estuary: regulation by light-limitation. Estuarine Coastal and Shelf Science 21: 711–725.

Perez, T., W. Joel & D. Burrage, 2006. Airborne remote sensing of the Plata Plume using STARRS. Sea Technology 47: 31–34.

Piola, A. R., E. J. D. Campos, O. O. Möller Jr., M. Charo & C. Martínez, 2000. The subtropical shelf front off eastern South America. Journal of Geophysical Research 105(C3): 6565–6578.

Piola, A. R., R. P. Matano, E. D. Palma, O. O. Möller & E. J. D. Campos, 2005. The influence of the Plata River discharge on the western South Atlantic shelf. Geophysical Research Letters 32: L01603.

Platt, T., C. L. Gallegos & W. G. Harrison, 1980. Photoinhibition of photosynthesis in natural assemblages of marine phytoplankton. Journal of Marine Research 38: 687–701.

Platt, T., H. Boeman, E. Devred, C. Fuentes-Yaco & S. Satthyendrananath, 2005. Physical forcing and phytoplankton distribution. Scientia Marina 60: 65–73.

Rodríguez-Graña, L. & L. R. Castro, 2003. Ichthyoplankton distribution off the Península de Mejillones (23°S), under variable hydrographic conditions in two seasons of the El Niño, 1997. Hydrobiologia 501: 59–73.

Saraceno, M., C. Provost & A. R. Piola, 2005. On the relationship between satellite-retrieved surface temperature fronts and chlorophyll a in the western South Atlantic. Journal of Geophysical Research 110: C11016.

Sournia, A., 1978. Phytoplankton Manual (Monographs on Oceanographie Methodology, 6). UNESCO, París.

Steeman-Nielsen, E., 1952. The use of radiactive carbon (^{14}C) for measuring organic production in the sea. Journal du Conseil International pour l' Exploration la Mer 18: 117–140.

Strickland, J. D. H. & T. R. Parsons, 1972. A Practical Handbook of Seawater Analyses. Bulletin of the Fisheries Research Board Canada.

Strom, S. L., M. A. Brainard, J. L. Holmes & M. B. Olson, 2001. Phytplankton blooms are strongly impacted by grazing in coastal North Pacific waters. Marine Biology 138: 355–368.

Sverdrup, H. U., M. Johnson & R. Fleming, 1942. The Oceans. Their Physics, Chemistry and General Biology. Prentice Hall, New York.

Thomsen, H., 1962. Masas de agua características del Océano Atlántico (parte Sudoeste). Servicio de Hidrografía Naval, Publ H632, Buenos Aires: 1–27.

Tomas, C. R., 1995. Identifying marine diatoms and dinoflagellates. Academic Press, Inc., San Diego, CA.

Wells, P. G. & J. R. Daborn, 1997. The Rio de la Plata, An Environmental Overview. An Ecoplata Project Background Report, Dalhousie University, Halifax, Nova Scotia, Canada: 256.

Wofsy, S. C., 1983. A simple model to predict extinction coefficients and phytoplankton biomass in eutrophic waters. Limnology & Oceanography 28: 1144–1155.

Yacobi, Y. Z., 2006. Temporal and vertical variation of chlorophyll a concentration, phytoplankton photosynthetic activity and light attenuation in Lake Kinneret: possibilities and limitations for simulation by remote sensing. Journal of Plankton Research 28: 725–736.